DTM 0232-1100

Final Report

for

Hybrid Capillary/Mechanically Pumped Loop Evaluation and Test

Prepared for

TSI Infosystems

(GSFC Contract NAS5-28626, Task 52)

Under Purchase Order No. DT3082

October 17, 1986

Dynatherm Corporation

1 Beaver Court

Cockeysville, Maryland 21030

1.0 INTRODUCTION AND SUMMARY

This report summarizes the work performed by Dynatherm Corporation, under subcontract to TS Infosystems, for the continued development of two phase heat transfer systems for large space structures. The program was concentrated in three major tasks: characterization of the baseline performance capabilities of a refurbished GFE capillary pumped loop, evaluation of a hybrid capillary/mechanically pumped loop, and the design of an increased capacity CPL.

The first two tasks were performed using the capillary heat transfer system (CHS) developed by Dynatherm for Goddard Space Flight Center under contract number NAS5-27122. Under the current subcontract, the CHS was refurbished and retested as a stand-alone capillary system. Its performance capabilities were found to be consistent with those previously established. The CHS was also fitted with a new liquid isolator which improved performance substantially.

A mechanical pump was also incorporated into the CHS in order to evaluate the behavioral characteristics of a hybrid capillary/mechanically pumped system. Parallel and series pump configurations were tested and the need for pump isolators was investigated. Under the conditions tested the results clearly indicate that the parallel pump configuration is the better choice, although additional testing is required to quantify performance augmentation. Series pump configurations can flood the capillary pumps and can result in temperature control problems. Pump failure in either hybrid configuration does not readily

spread to other pumps. Hence, isolators may not be required for hybrid systems, unless of course, a potential operating scenario for the hybrid system is a capillary pump stand-alone mode.

The third task evaluated the feasibility of higher performance CPLs. Based on the test results obtained in Task 1, CPL performance capabilities appear to be consistent with next generation NASA design requirements of 450 kW-meters. With an improved isolator design like the one tested during the first task, and with increased transport line size, minor modifications to the evaporator pump should allow pump length to increase up to about a meter and total system load to increase to 15 kW.

2.0 TECHNICAL DISCUSSION

2.1 Background

During a previous program performed for Goddard Space Flight Center under contract number NAS5-27122, Dynatherm designed, fabricated and tested a capillary heat transport system (CHS). The CHS incorporated two capillary pumps, liquid and vapor transport lines, a condensing cold plate, a liquid subcooler, a reservoir and a liquid isolator. The capillary pumps were distinctly different in their design. One pump incorporated vapor channels formed by axial grooves in the aluminum pump body. In the other pump, the vapor channels were formed by axial grooves machined in the Porex insert. The CHS, which is shown schematically in Figure 1, is described fully in the final report, DTM 0218-1101, submitted under the previous program.

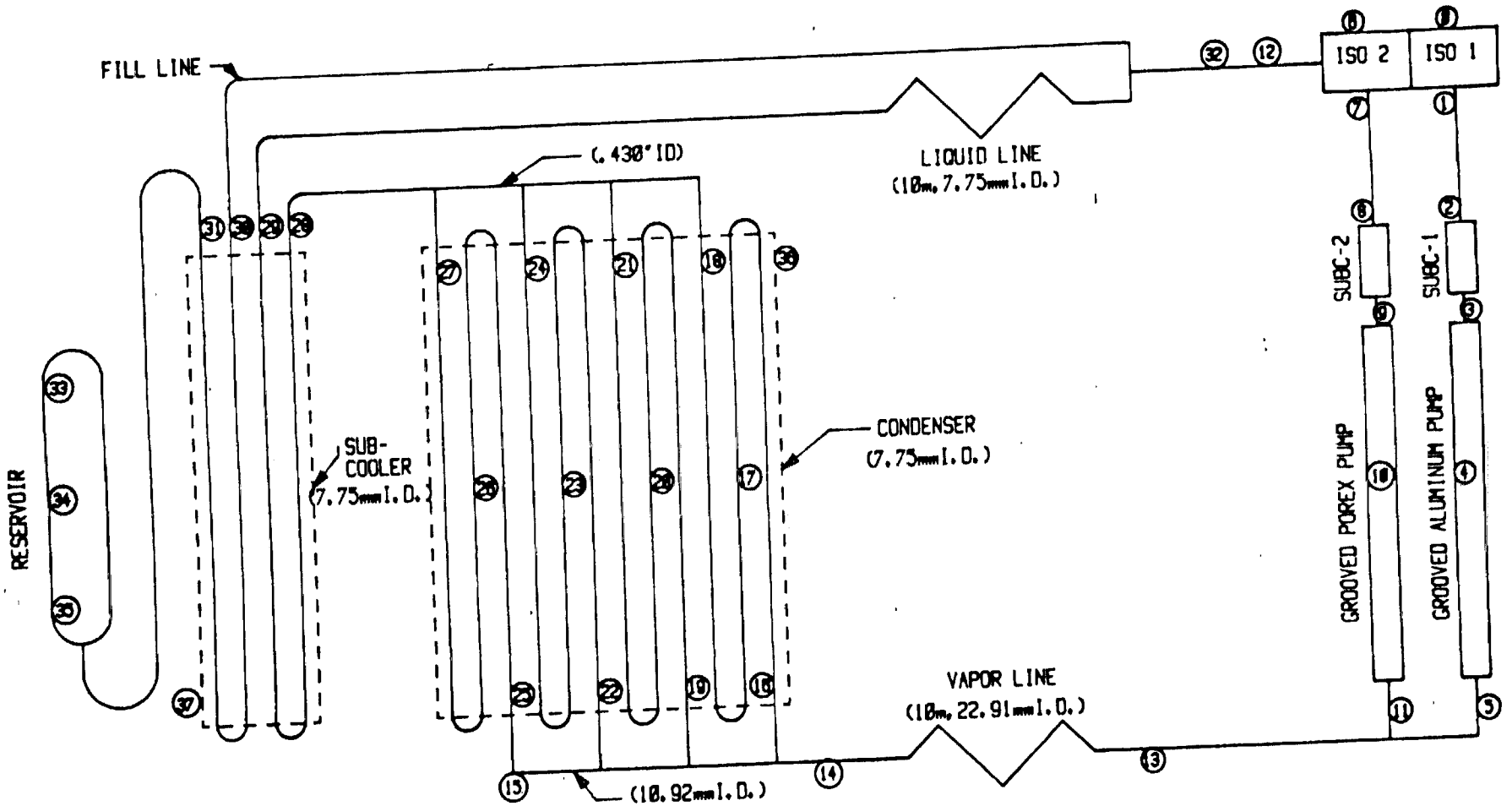

CAPILLARY PUMPED LOOP

GSFC/DYNATHERM

Figure 1

During that program, the CHS was performance tested to establish heat transport capability and conductance of the pumps and their heat load sharing capability. Tests were also conducted to demonstrate the temperature control characteristics of the reservoir and proper behavior of the liquid isolator. Although some of the tests were limited by practical restraints such as limits of the electrical heaters and the capacity of the refrigerated cooling bath, all design requirements were met. Total system heat transport as high as 2400 watts was achieved with individual pump loads as high as 1500 watts.

The current program, which was divided into three tasks, used the existing CHS as a test vehicle. The first task involved refurbishment of the CHS and additional testing to further characterize its performance. During the second task, the CHS was fitted with a mechanical pump and tested as a hybrid capillary/mechanically pumped loop. The third task evaluated the feasibility of increasing CPL capacity. The program effort devoted to each of these tasks is detailed in the following sections.

2.2 Task 1 - Refurbishment and Retest of CHS

2.2.1 Refurbishment of CHS

The CHS was fitted with a new reservoir with greater fluid capacity than the previous reservoir. The new reservoir was made from a one-gallon stainless steel sample cylinder. Each end of the cylinder was sealed with a welded plug which terminated in valved 9.5 mm (.375 inch) diameter lines. Cooling coils were soldered to the top 20 cm (8 inches) of the reservoir and Minco

heaters were attached to the lower 10 cm (4 inches). The reservoir was mounted in a near vertical position with its upper end approximately 18 cm (7 inches) below the CHS condenser. The reservoir was charged with 1930 grams of electronic grade ammonia and then attached to the loop via the valved port at its bottom.

The capillary pump heater blocks were also reworked. These heater blocks contain cooling channels to enable them to serve as heat sinks during heat load sharing tests. Some external plumbing for the cooling channels was removed to allow the heater blocks to be shortened. This allowed the heaters to be attached to the pump body at an axial position farther downstream from the liquid-vapor seal inside the pump. Previous test results indicated that vaporization occurred on the wrong side of the liquid-vapor interface. The movement of the heater as described above reduced this tendency.

The CHS was also reinstrumented and reinsulated. Copper constantan thermocouples were attached at those positions shown in Figure 1. All liquid and vapor transport lines were individually wrapped with closed cell neoprene insulation. The capillary pumps, the reservoir and the condenser were not insulated.

2.2.2 CPL Stand-Alone Tests

Testing was initiated in the first week of May 1986. Test plans were initially formulated to compare current CHS performance to the previous test results. The plans called for testing each pump to its heat transport limit with the other pump loaded at low power (200 watts), and then operating both pumps to their performance limits simultaneously. During the course of the

tests the adverse elevation of the CHS was varied between 6 cm and 50 cm (2.5 and 21.5 inches), measured from lowest point in condenser to the centerline of the capillary pump.

Table 1 presents a summary of the test results. The initial tests were conducted at an adverse elevation of 6 cm. The results are consistant with those obtained during the previous program. The grooved aluminum pump demonstrated a heat transport limit of 1800 watts with the grooved Porex pump powered at 200 watts. The grooved Porex pump heat transport limit was determined to be 1200 watts with the grooved aluminum pump powered at 200 watts. Temperature gradients measured between the pump body (TC 4 or 10 in Figure 1) and the CHS reservoir (TC 34 in Figure 1) are shown in Figure 2 as a function of power. The failure mode observed on both pumps consisted of a gradual increase in this temperature gradient with time, which is indicative of local dryout of the pump's wick structure and not a total deprime. This conclusion is further supported by the fact that pump recovery could be achieved by simply reducing power. Pressure priming, accomplished by lowering pump temperature below reservoir temperature, was not necessary.

Heat transport limits were also established by powering both pumps simultaneously. In all cases the grooved Porex pump was the first to fail. For example, both pumps could be powered simultaneously to 1000 watts, but increasing power to both pumps to 1100 watts caused failure of the grooved Porex pump. Table 1 summarizes measured heat transport limits during several simultaneous load tests. The highest combined heat transport for both pumps was 2600 watts.

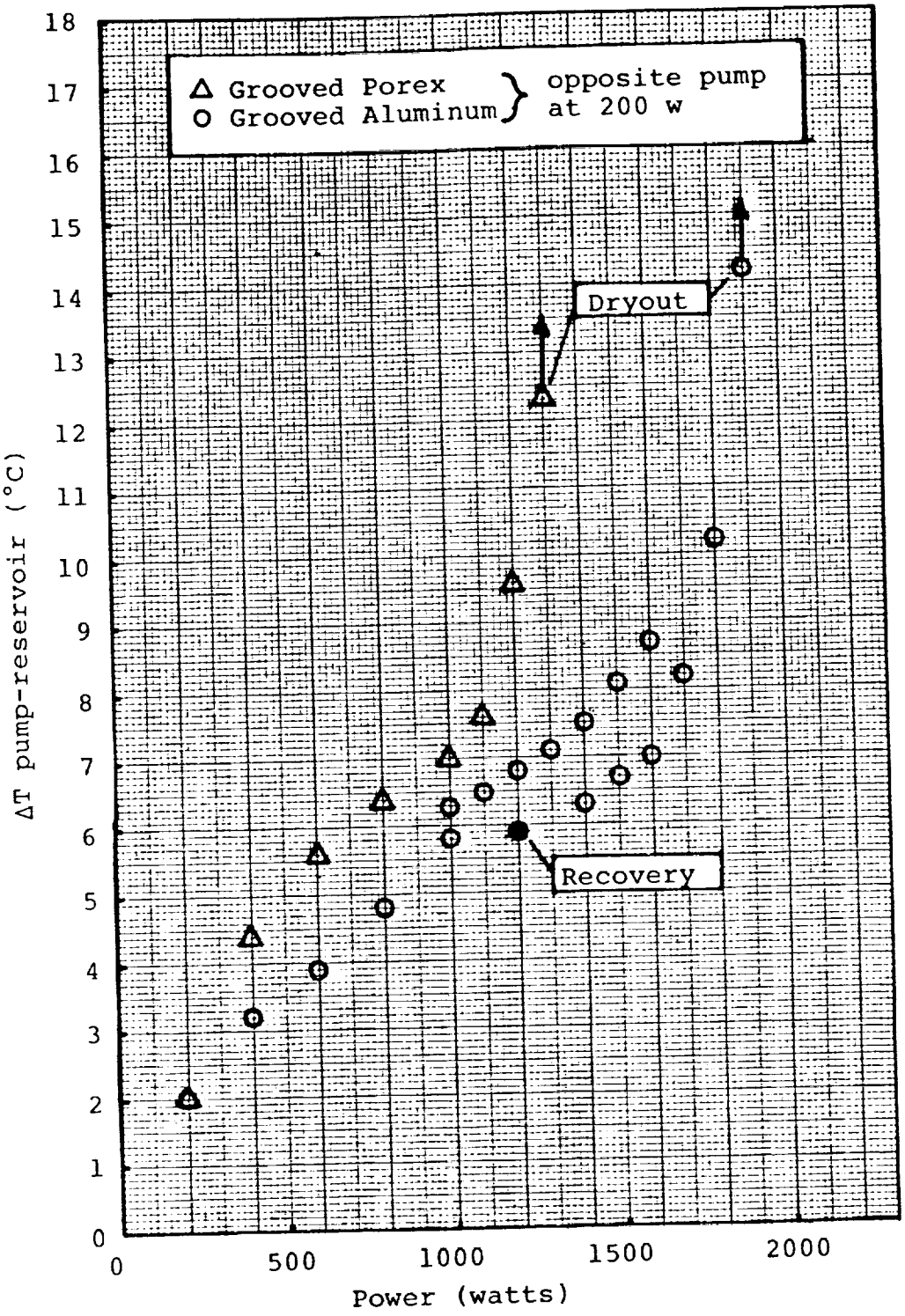

Figure 2
Temperature Gradient vs. Power
(Original Isolator/Pump Pairs)

Table 1

Test Summary for CPL Stand-Alone Tests

(Original Isolator/Pump Pairs)

Type of Test	Elevation (cm)	Grooved Aluminum Heat Input(w)	Grooved Porex Heat Input(w)
Peak Pump Load (opposite pump at 200 w)			
	6	1800	200
	6	200	1200
Simultaneous Pump Loads			
	6	1400	1000
	6	1800	800

Pressure distribution through the loop was determined for several of the tests shown in Table 1. The analysis shows that the liquid isolator is responsible for a substantial portion of the total pressure drop. Unfortunately, the magnitude of the pressure drop depends heavily on several assumptions concerning the isolator geometry. Figure 3 shows a schematic of the liquid isolator. It consists of a thick Porex membrane surrounded by a small annular gap which feeds the liquid entrance of the pump. Due to the smallness of the annular gap, small variations in its size, on the order of a half a millimeter, have a large effect on the pressure drop.

The pressure drop analysis of the isolator does bear out one important point. Vendor data on the permeability of Porex shows considerable spread. Scaling original vendor data from a filtration size of 35 u to 10 u while assuming permeability is

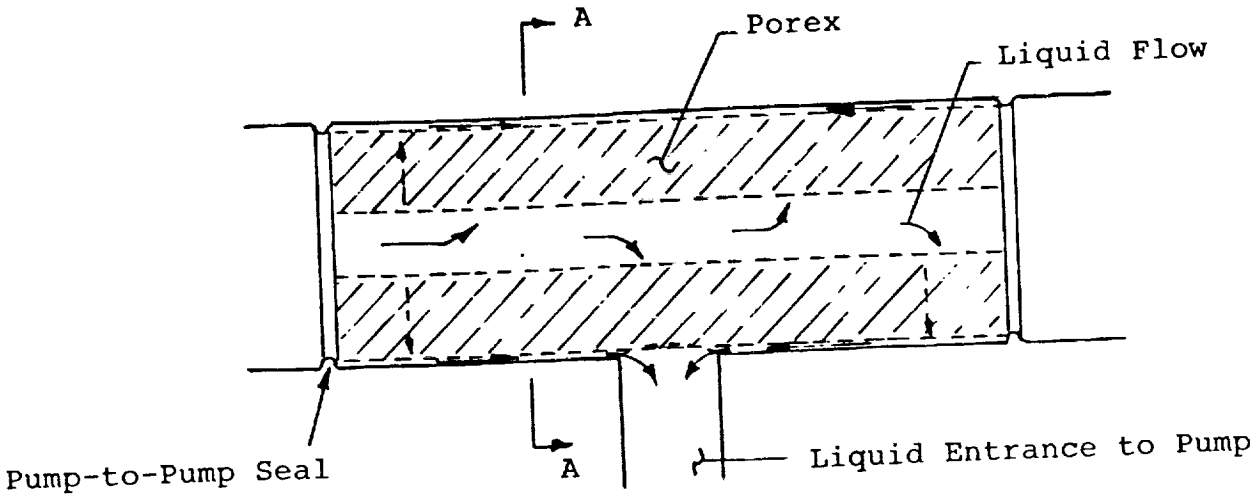

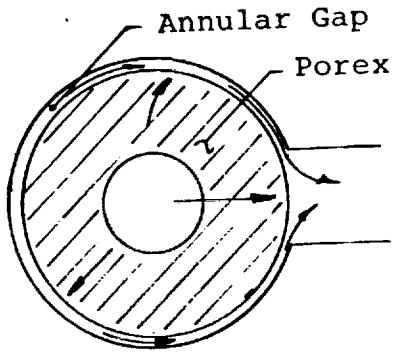

Section A-A

Figure 3

Schematic of Isolator

proportional to pore size squared, the permeability of the 10 u Porex used in the isolator should be 1.8×10^{-13} m^2. Scaling more recent vendor data in the same manner, the permeability is an order of magnitude higher.

Because of the questions regarding Porex permeability and its considerable influence on loop performance, Dynatherm performed its own tests to establish permeability. Tests were performed with methanol at room temperature. The test measurements indicate a permeability of 1.55×10^{-12} m^2 which support the more recent vendor data. The higher permeability also agrees better with the CHS test data. If the lower permeability is used in the pressure analysis, the pressure drop in the liquid isolator wick alone is nearly equal to the total capillary head developed by the pump, which leaves no head to overcome other system pressure drops.

The grooved aluminum pump performed better than the grooved Porex pump in all tests performed during the previous program and in all tests summarized in Table 1. In order to further compare the pumps, the isolator/pump pairs were switched. This was achieved by crossing the lines connecting each pump to the isolator, thereby connecting the grooved aluminum pump to the isolator section previously used for the grooved Porex pump and vice versa. Tests conducted in this fashion clearly indicate that the grooved Porex pump actually performs better than the grooved aluminum pump. Test results from these tests are summarized in Table 2. The grooved Porex pump was powered without failure to the power limit of the heater, 2000 watts, compared to a 1200 watt limit when tested with the other isolator (see Table 1).

The grooved aluminum pump on the other hand could only be powered to 900 watts, compared to 1800 watts previously.

The fact that the grooved Porex pump performs better than the grooved aluminum pump may give some indication as to the nature of the pump's performance limit. The grooved aluminum pump offers lower flow resistance than the grooved Porex pump in both the liquid and vapor phases. Also, during bubble testing prior to installation, its capillary pumping head was determined to be slightly better than the grooved Porex pump. The grooved Porex pump on the other hand offers greater surface contact area between the pump body and the wick structure. This would indicate that the measured pump limits are flux dependent (possibly boiling limited) and not related to capillary pumping limits.

Since heater limits prevented the characterization of the heat transport capability of the grooved Porex pump, additional tests were performed at increased elevation. Tests were performed at adverse elevations as high as 55 cm (21.5 inches). Measured performance is shown as a function of elevation in Figure 4. The performance degradation with increased elevation is not nearly as large at it should be. According to bubble tests performed with ethanol on the pumps during the previous program, the pump's equivalent static height with ammonia is on the order of 64 cm (25 inches). Extrapolating the tests points for the grooved Porex pump indicates a static height of nearly 140 cm (55 inches). Again, this discrepancy may be related to the nature of the measured heat transport limits. The pump failure modes are not catastrophic but rather are characterized

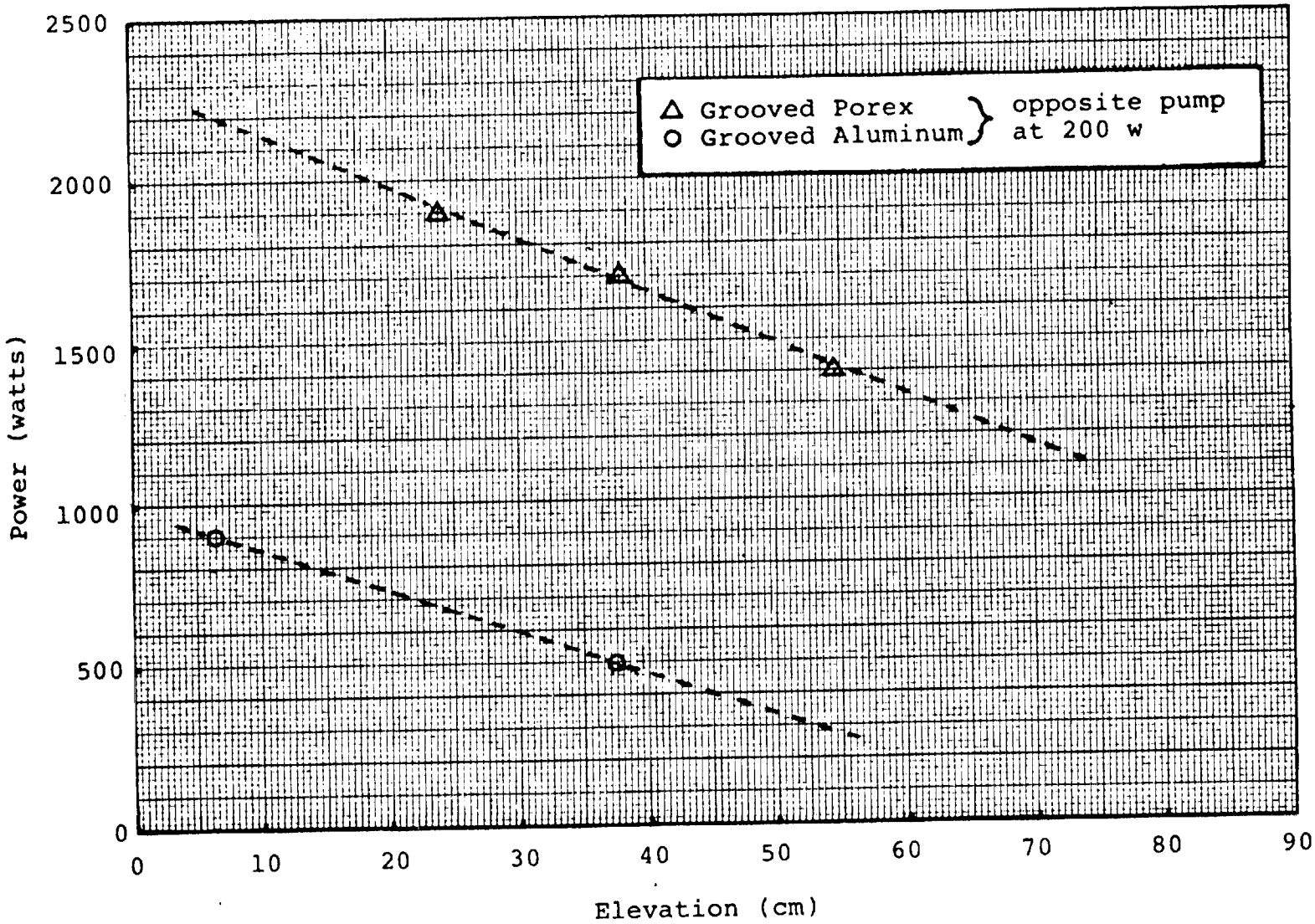

Figure 4
Performance vs. Elevation
(Switched Isolator/Pump Pairs)

by gradual increases in the pump's temperature. This suggests that the measured limits may be flux dependent and hence not affected by adverse elevation in the same manner as a transport limit.

Table 2

Test Summary for CPL Stand-Alone Tests

(Switched Isolator/Pump Pairs)

Elevation (cm)	Grooved Aluminum Heat Input (watts)	Grooved Porex Heat Input (watts)
6	900	200
38	500	200
6	200	2000*
24	200	1900
38	200	1700
55	200	1400

* heater limit

Following these tests, a new isolator section was designed and fabricated. The new design which is shown in Figure 5, improved on the old isolator in two ways. First, it incorporated a large 1.1 mm (0.045 inch) annular gap outside the Porex membrane. A gap of this size contributes negligibly to the total isolator pressure drop. Secondly, the thickness of the Porex was reduced to 1.3 mm (0.050 inch). The new isolator was tested for pressure drop prior to installation in the CHS. Tests were

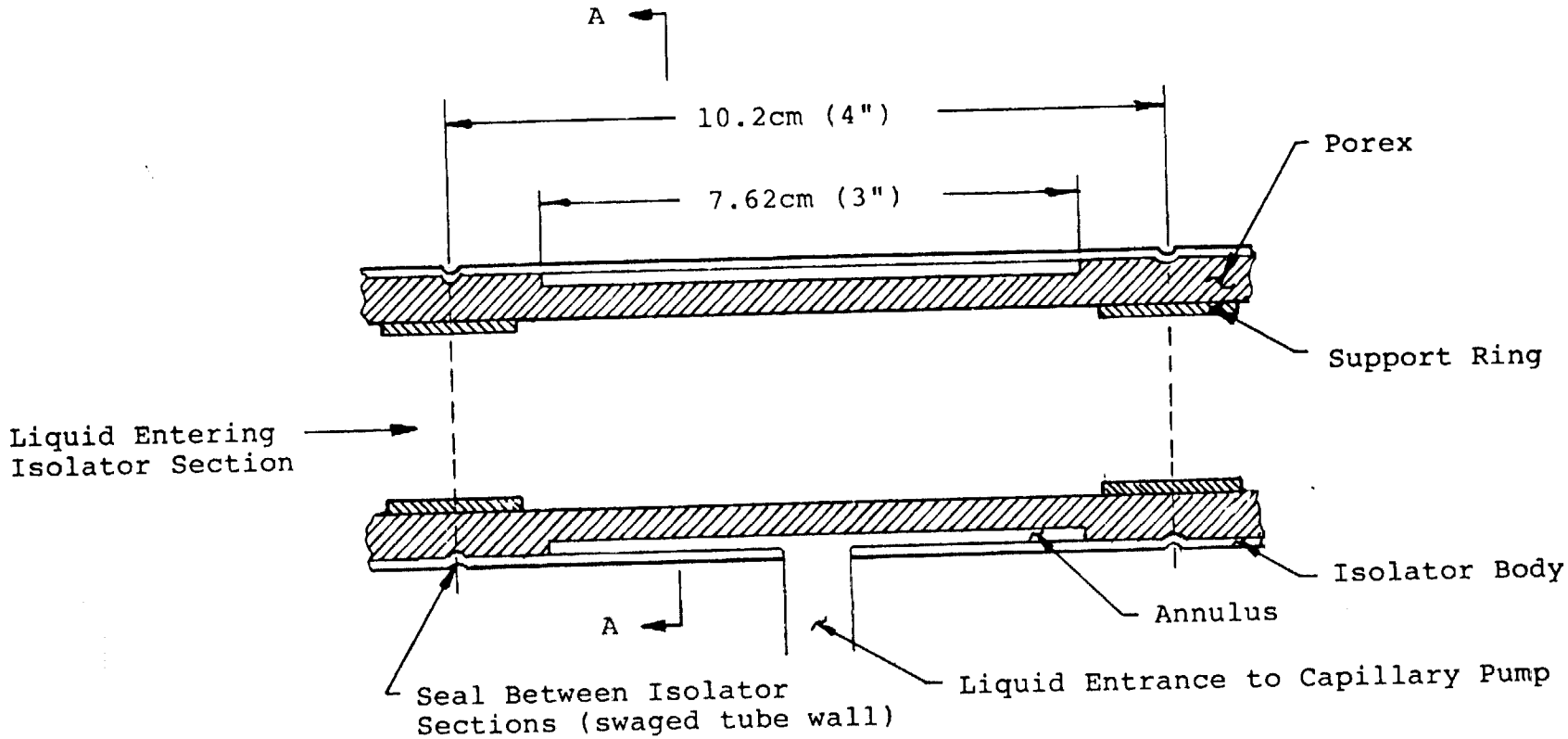

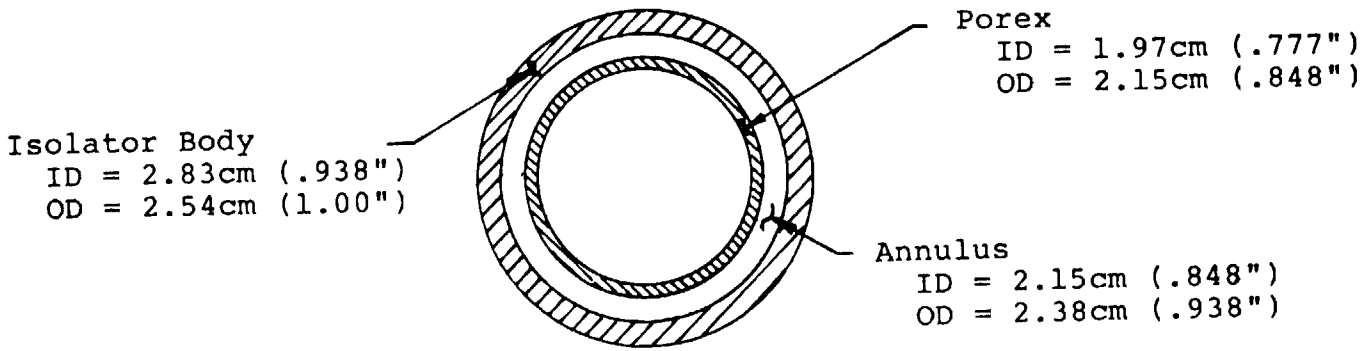

Section A-A

Figure 5

New Isolator Design

performed with methanol at room temperature. The old isolator was also tested after removal from the CHS. The results emphasize two important points. First, the old isolator shows an order of magnitude difference in flow resistance between the two sections used during the CHS tests. This explains the vast difference in the performance of each pump when the pump/isolator pairs were switched. Second, the new isolator improves the flow resistance by a factor of 7.5 over the best section in the old isolator.

The new isolator was installed in the CHS and the performance tests were repeated. At an adverse elevation of 24 cm (9.5 inches) both pumps were powered to the heater limit (2000 watts) with the other pump powered at 200 watts. The pumps were also powered simultaneously to a total power of 3600 watts without failure. Limitations of the refrigerated bath precluded testing at higher power. Tests were performed at higher elevations to circumvent heater and refrigerated bath limitations. At 55 cm (21.5 inches), the CHS was run stably with a total load of 2400 watts (1400 watts on the grooved Porex pump and 1000 watts in the grooved aluminum pump).

2.3 Task 2 - Hybrid Capillary/Mechanically Pumped Loop

2.3.1 CHS Hybrid Modifications

At the same time the new isolator was installed in the CHS, other modifications were incorporated to facilitate hybrid testing. The modifications included the addition of a magnetically driven pump, additional liquid line to couple the mechanical pump

to the existing loop, and a multitude of valves to enable series and parallel mode hybrid tests.

A layout of the hybrid system is shown in Figure 6. The pumped leg was basically coupled to the loop in parallel with the existing liquid line. At the condenser end of the loop, the mechanically pumped leg was tied into the midpoint of the liquid subcooler in order that subcooling would be available to both the existing liquid line and the pumped liquid line. At the opposite end of the loop, the mechanically pumped leg was tied in on either side of the liquid isolator.

Four stainless steel ball valves with TFE packing were incorporated in the positions shown. These valves allowed CHS testing in a CPL stand-alone mode, with the mechanical pump and the capillary pumps in series, and with the mechanical and capillary pumps in parallel. The liquid isolator could be bypassed in all operating modes.

The mechanical pump was a stainless steel magnetically driven gear pump manufactured by Micropump (model no. 183). The pump has carbon graphite gears and a teflon static shield. The pump is driven by a variable speed DC motor (model no. 346). Maximum pump output is 725 cc/min which is equivalent to the liquid flow rate for an 8000 watt thermal load at 35°C.

2.3.2 Hybrid Tests

Testing was initiated on the hybrid system on May 28, 1986. Tests in the CPL stand-alone mode are those which were described earlier with the new isolator.

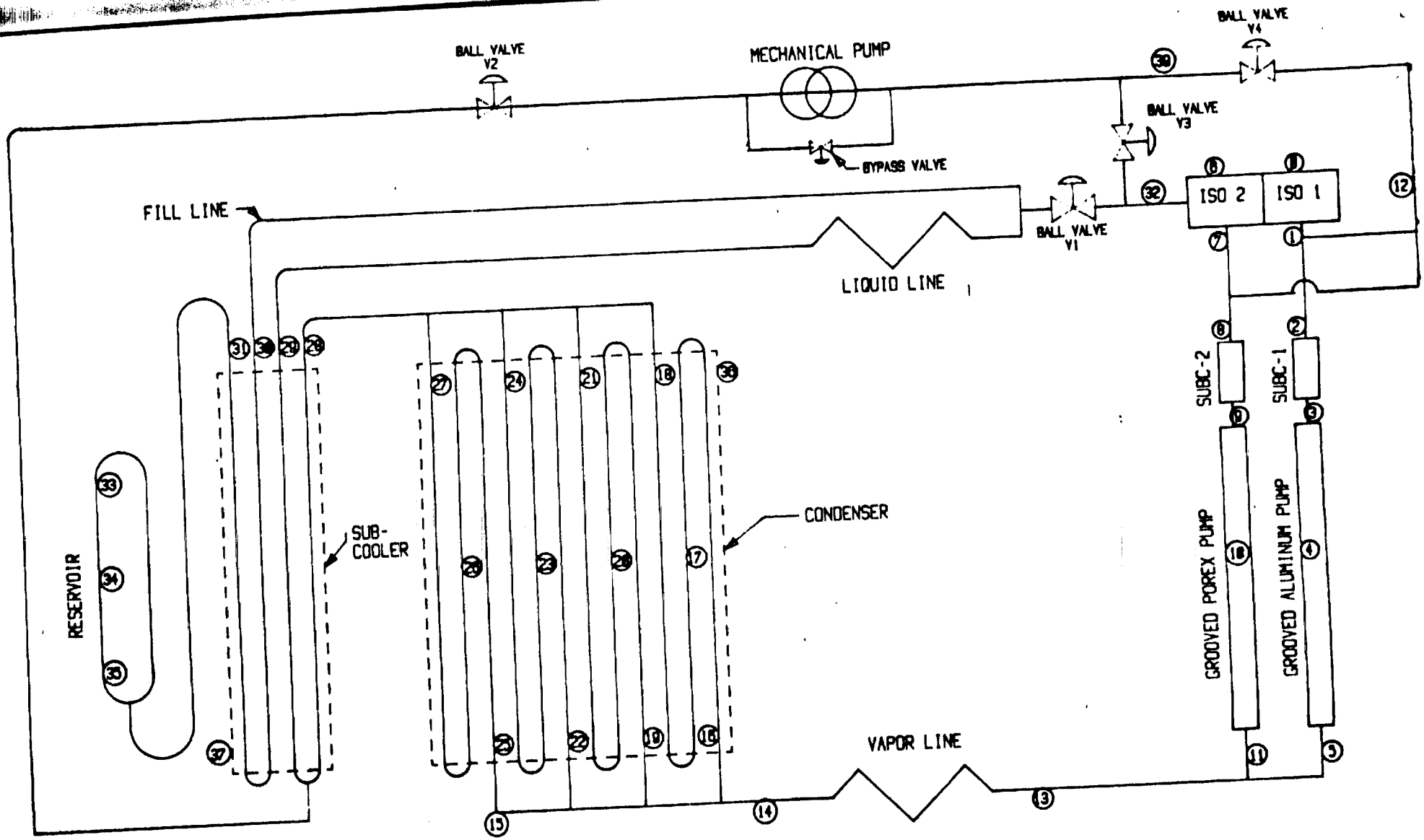

CAPILLARY PUMPED LOOP

GSFC/DYNATHERM

Figure 6

2.3.2.1 Series Configuration Tests

Tests with the mechanical pump and the capillary pumps in series were first conducted with the mechanical pump run at maximum speed. This results in a liquid flow rate through the mechanical pump, and hence the capillary pumps, which corresponds to a thermal load in excess of 8 kw. Under these operating conditions several things occur. First, the reservoir deprimes. Pump suction pulls all liquid out of the reservoir which eliminates temperature control of the loop normally afforded by temperature control of the reservoir. Secondly, the quality of the flow at the exit of the capillary pumps can vary between single phase liquid and single phase vapor depending on heat load. As a result, an unpowered capillary pump receives subcooled liquid from the condenser and is maintained at subcooled liquid temperature, not saturation conditions. Saturated conditions can be maintained at the capillary pump only when the heat input is sufficient to heat the incoming liquid to the saturation temperature.

Series tests with and without isolator bypass showed distinct differences; however, they were related to the plumbing and not any inherent problem with a series flow arrangement. When the isolator was bypassed (V4 open, V3 closed) there was no tendency for capillary pump failure to affect other pumps. However, when the liquid flow passed through the isolator (V3 open, V4 closed), purposely failing one capillary pump quickly led to the failure of the other pump. The U-tube shown in Figure 6 as part of the liquid line leading from V4 to the capillary pumps

provides an additional path for communication between the pumps which does not go through the isolator. This problem was later rectified by moving valves V2 and V4 to the positions shown in Figure 7.

Series tests were also performed at variable mechanical pump speed. During these tests only one of the capillary pumps was powered (grooved Porex). Power on the grooved Porex pump was kept constant at 1500 watts and the mechanical pump speed was gradually decreased until dryout occurred. During the entire test the unpowered pump ran at subcooled liquid temperature. The grooved Porex pump dried out when the pump speed fell below 2500 rpm which corresponds to a liquid flow rate corresponding to a thermal load of about 2800 watts, approximately twice the system load. It appears that the total mechanical pump flow rate is split evenly between the pumps. This implies that in a series configuration which uses variable pump speed to adjust flow, the required mechanical pump flow rate is determined not by total system load but by the flow requirements for the highest loaded capillary pump.

With substantial liquid flow rates through unpowered capillary pumps, heat load sharing in the series flow configuration is impossible. Vapor generated in powered capillary pumps will be swept by the liquid toward the condenser and never given a chance to condense in the unpowered pumps.

2.3.2.2 Parallel Configuration Tests

Tests with the mechanical pump in parallel with the capillary pumps yielded considerably different results. The two major

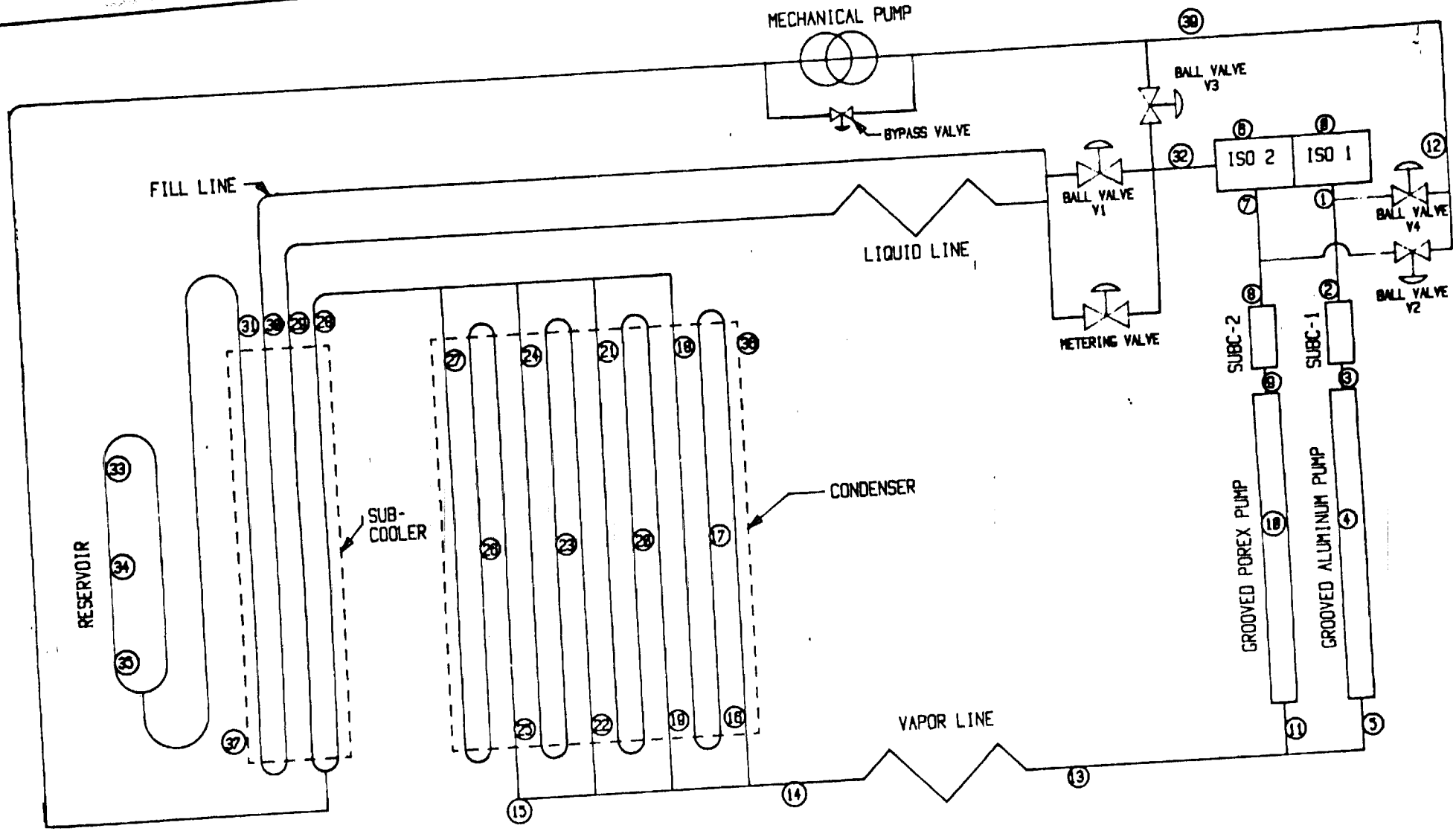

CAPILLARY PUMPED LOOP

GSFC/DYNATHERM

Figure 7

problems which are characteristic of the series configuration, namely reservoir depriming and capillary pump flooding, are not nearly as prevalent in a parallel mode.

Consider the simplified schematic of a parallel hybrid configuration shown in Figure 8a. The total flow resistance of the CHS is represented by two components, a liquid-side resistance, R_l, and the balance of the total resistance in the capillary loop, R_v. The total flow rate through the mechanical pump is $\dot{m}_p$ and the flow rate through the capillary pumps is $\dot{m}_v$. It can be shown that $\dot{m}_v$, which actually represents heat transport capacity of the system, is given by the equation

$$\dot{m}_v = \frac{\Delta P_{cp}}{R_v + R_l} + \dot{m}_p \frac{R_l}{R_v + R_l}$$

where $\Delta P_{cp} = \frac{2\sigma}{r_p}$ = pumping developed by capillary pumps.

The first term on the right hand side of the equation is the flow which is normally supplied by the CPL stand-alone system and the second term is the augmentation provided by the mechanical pump. As one might expect, the augmentation is proportional to the mechanical pump flow rate. However, it also depends on the resistance distribution. The greater the relative resistance in the liquid phase, the greater the augmentation afforded by the mechanical pump.

The pumping developed by the capillary pumps, ΔP_{cp}, can vary anywhere between zero and ΔP_{cap}, the pumping capability of the capillary pumps. Figure 8b shows two curves which define the acceptable range of performance for a parallel hybrid system. The lower curve represents a flooding limit which occurs when

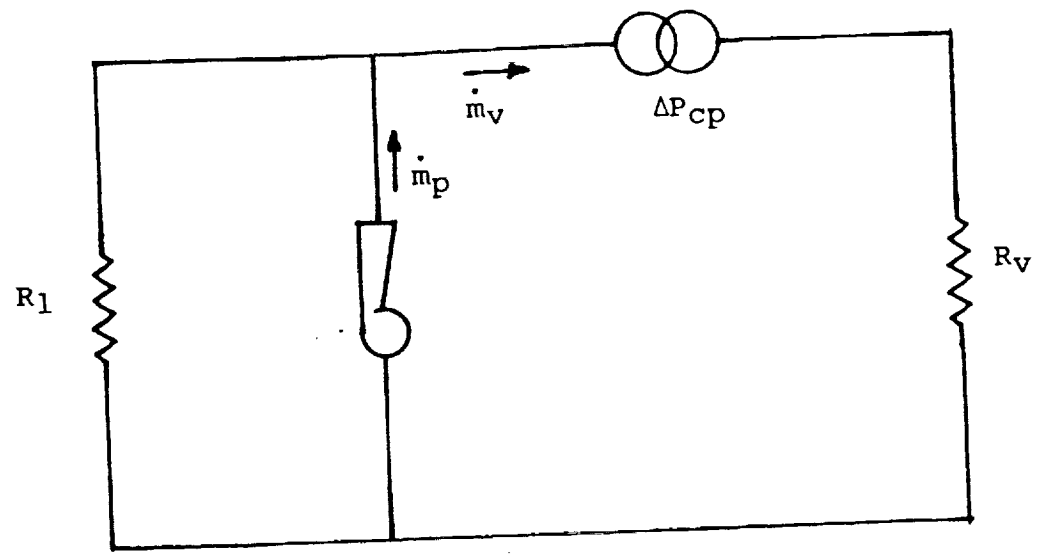

8a. Schematic of Parallel Pump Configuration

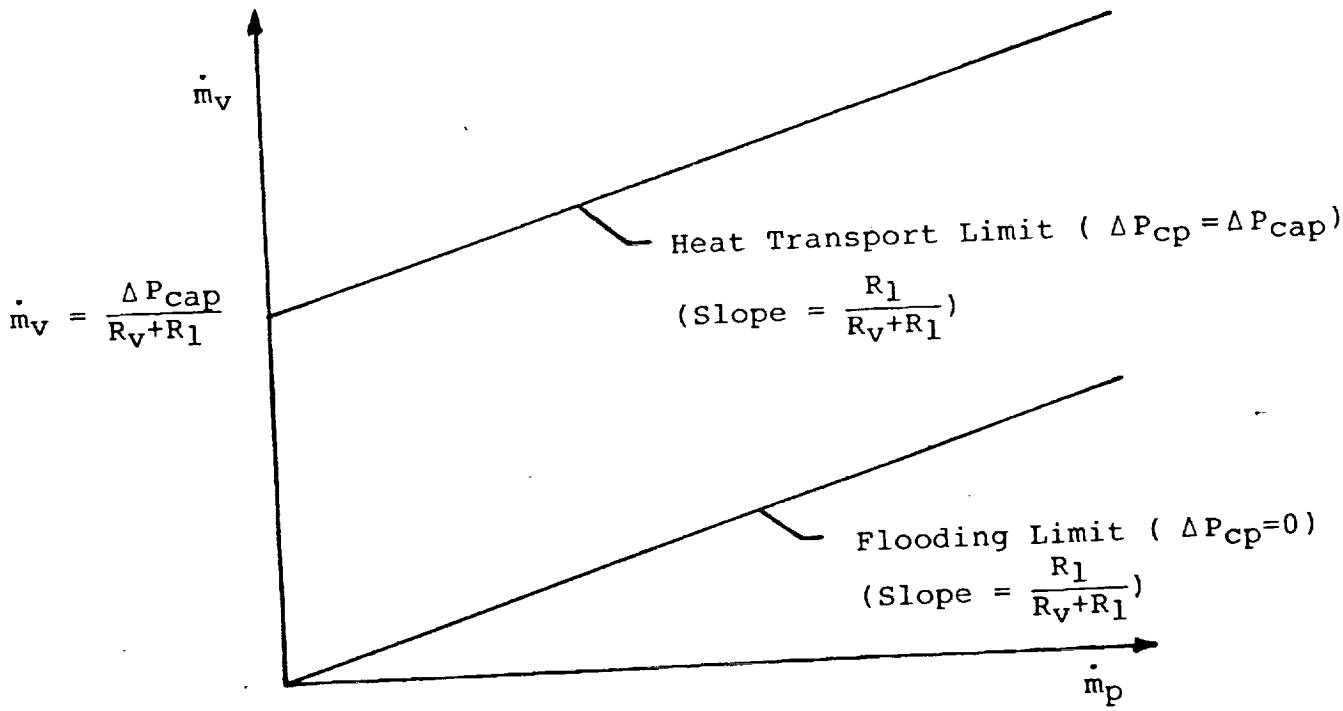

8b. Performance Range for Parallel Pump Configuration

Figure 8

that portion of the total flow rate which passes through the capillary pumps, $\dot{m}_p(R_l/(R_v + R_l)$, is too large for the flow rate demanded by the system heat load, $\dot{m}_v$. The upper curve represents the heat transport limit, which occurs when the pumping developed in the capillary pumps is equal to the pump's capability. The vertical separation between the two curves, which represents the variation in system heat load (actually $\dot{m}_v/\lambda$) which the parallel hybrid system can tolerate, is equal to the capacity of the CPL stand-alone system ($\Delta P_{cap}/(R_v + R_l)$).

Parallel hybrid configuration tests were performed over a wide range of conditions. For the most part, the tests were performed at elevations between 24 and 55 cm (9.5 to 21.5 inches) in order to limit heat transport capability to levels compatible with heater and refrigeration system limitations. Pump power was varied between 200 and 2000 watts/pump.

The test results support the wide variability in allowable system load which is indicated in Figure 8. At all pump powers in the test range, the temperature distribution throughout the loop in the parallel mode is similar to that of a CPL stand-alone system. In all tests except one which is discussed later, pump flooding and reservoir depriming was nonexistent. Even unpowered pumps run at saturation conditions, not at subcooled liquid temperature as in the series mode tests.

Since the parallel mode offered these attractive operating features, a considerable amount of test effort was devoted to characterizing the augmentation afforded by the mechanical pump. Initially, the performance enhancement could only be characterized at high elevation since heater limits prevented the determi-

nation of CPL stand-alone limits at low elevation. At an adverse elevation of 55 cm, the performance in the CPL stand-alone mode was determined to be 2400 watts. In the parallel mode, with the mechanical pump powered fully, the measured performance increased to 2800 watts.

In order to investigate augmentation at lower elevation, a metering valve was installed in parallel with valve V1 as shown in Figure 7. At the same time, the grooved Porex pump was removed from the loop because of problems which will be discussed later. After the metering valve was installed all tests were conducted at an adverse elevation of 24 cm (9.5 inches).

With the metering valve fully open, the performance of the grooved aluminum pump in a CPL stand-alone mode exceeded the heater limit (2000 watts). The metering valve was then adjusted until the CPL stand-alone capability was 1500 watts. Then with the metering valve in the same position, the mechanical pump was powered and attempts were made to establish the heat transport limit. As it turned out, the augmentation provided by the mechanical pump allowed the grooved aluminum pump to be powered to the heater limit (2000 watts) without failure. At the same metering valve position and pump speed, the capillary pump flooded when the heat input was reduced to 500 watts. These results are consistent with Figure 8b in that the offset between the heat transport limit and the flooding limit is equal to the CPL stand-alone capacity (1500 watts at this metering valve setting which is also the difference between 2000 and 500 watts).

Another interesting point to be made about the above tests is the variation in the amount of augmentation provided by the mechanical pump. At an adverse elevation of 55 cm, the mechanical pump increased performance by 17% (2400 to 2800 watts). At an elevation of 24 cm, the mechanical pump increased performance by 33% (1500 to 2000 watts). The difference in augmentation is not attributable to the difference in elevation, but to the difference in liquid-side resistance. At the lower elevation, the metering valve was partially closed in order to reduce capacity to 1500 watts. Refering to the equation on page 21, the amount of augmentation provided by the mechanical pump, $\dot{m}_p(R_l/(R_v + R_l))$, increases as the liquid-sink resistance increases. This conclusion is supported by the above tests.

As previously mentioned, problems developed with the grooved Porex pump during the hybrid testing. At one time the measured pump performance exceeded the heater limit of 2000 watts; however, during the latter stages of the hybrid tests, pump limits on the order of 700 to 1000 watts were measured. The grooved Porex pump was removed from the loop and subjected to a series of inspections and tests to diagnose the problem. Bubble tests on the pump indicated that its pumping was substantially lower, about 1/3 of its value prior to installation. Further investigation showed that the pump contained several contaminants which included translucent gummy deposits in the liquid entrance to the pump and fine black deposits on the pump's Porex wick structure which showed obvious signs of stratification.

Probably most important, however, was the fact that the Porex wick structure had shifted axially relative to the pump

body nearly 4 cm (1.5 inches) from its original position in the direction of the vapor manifold. It is postulated that the pressure developed by the mechanical pump was responsible for this movement. The axial movement could have been responsible for the change in pumping head experienced by the pump. The movement also affected the temperature of the subcooled liquid entering the pump. The liquid-vapor seal at the pump's entrance was actually shifted to a position under the pump's heater allowing heat input on the liquid side of the seal.

Axial movement can be prevented quite easily on future grooved Porex pumps. A counterbored step in the aluminum pump body similar to the one used on the grooved aluminum pump can be incorporated to mate with a step machined in the Porex insert.

2.4 Task 3 - Increased Capacity CPL

The third task of the current program was devoted to the evaluation of the feasibility of increasing CPL capacity. Next generation requirements include a system capacity of 15 kilowatts, transport distances of 30 meters and cold plate configurations which utilize 0.9 meter (3 foot) long pumps.

Toward this objective a design analysis was conducted with the following objectives:

- o characterize pressure distribution in the existing CPL at current load levels
- o identify CHS component design modifications necessary to maintain pressure drops at current levels for increased system capacity

Provided this second objective can be achieved, the capillary pumping which the current pumps provide will be sufficient for increased capacity systems and hence the Porex used in the current pumps can also be used in next generation pumps.

In the evaluation of CHS pressure distribution it is best to segregate the loop into components whose pressure drops are related to either total heat load or to the heat load per pump. For instance, the pressure drop in all liquid and vapor transport lines and the condenser depend on total heat load whereas the pressure drop through the isolator and the capillary pump depend on pump heat load.

Table 3 summarizes the major component pressure drops for the current CHS at a total system load of 6 Kw and a pump heat load of 1.5 Kw. The grooved Porex pump geometry was used to evaluate pump pressure drop and the best isolator section of the original isolator was used to evaluate isolator pressure drop. The table clearly indicates that the vapor channels in the capillary pump and the isolator are the two major sources of pressure loss in the CHS.

A new isolator design was fabricated and tested under Task 1 which offers substantial improvements in pressure drop over the original design. The new isolator incorporates two major design changes. First, the thickness of the Porex membrane in the isolator was reduced to 1.3 mm (.050 inch) from a previous value of 5.9 mm. Second, the annular gap between the Porex and the stainless steel isolator body was increased to 1.1 mm (0.045 inch). Bench tests on the new isolator showed that its flow resistance was 7.5 times lower than the best isolator section in

Table 3
Component Pressure Drop for Current CHS
(Q_{Total} = 6000 watts, Q_{pump} = 1500 watts)

Component	Equation		Re	$\Delta P(N/m^2)$
	Laminar	Turbulent		
Pump				
Vapor	$\frac{20.37\ Le\ \nu_v\ Q_p}{D_{ve}^4\ Ne\ \lambda\ \rho_v}$	$\frac{0.0876\ Le\ \nu_v^{0.25}}{D_{ve}^{4.75}\ \rho_v}\left(\frac{Q_p}{\lambda\ Ne}\right)^{1.75}$	2260	632
Liquid	$\frac{\nu_l\ Q_p\ \ln(D_o/D_i)}{2\ \P\ Le\ K\ \rho_l\ \lambda}$		Laminar	83
Isolator	$\frac{\nu_l\ Q_p\ \ln(D_o/D_i)}{2\ \P\ L_i\ K\ \rho_l\ \lambda} + \frac{5.09\ L_i\ \nu_l\ Q_p}{(D_o^2-D_i^2)(D_o-D_i)^2\ \lambda}$		Laminar	1000
Adiabatic				
Vapor	$\frac{40.74\ L_{va}\ \nu_v\ Q_t}{D_{va}^4\ \rho_v}$	$\frac{0.241\ L_{va}\ \nu_v^{0.25}}{D_{va}^{4.75}\ \rho_v}\left(\frac{Q_t}{\lambda}\right)^{1.75}$	24410	123
Liquid	$\frac{40.74\ L_{la}\ \nu_l\ Q_t}{D_{la}^4\ \rho_l\ \lambda}$	$\frac{0.241\ L_{la}\ \nu_l^{0.25}}{D_{la}^{4.75}\ \rho_l}\left(\frac{Q_t}{\lambda}\right)^{1.75}$	6120	367
Condenser (50% active)	$\frac{20.37\ L_c\ Q_t}{N_c\ \lambda\ D_c^4}\left(\frac{\nu_l}{\rho_l}+\frac{\nu_v}{\rho_v}\right)$	$\frac{.121\ L_c}{D_c^{4.75}}\left(\frac{Q_t}{\lambda\ N_c}\right)^{1.75}\left(\frac{\nu_l^{0.25}}{\rho_l}+\frac{\nu_v^{0.25}}{\rho_v}\right)$	1530(l),18040(v)	96
Subcooler	$\frac{40.74\ L_r\ \nu_l\ Q_t}{D_r^4\ \lambda\ \rho_l}$	$\frac{0.241\ L_r\ \nu_l^{0.25}}{D_r^{4.75}\ \rho_l}\left(\frac{Q_t}{\lambda}\right)^{1.75}$	6120	100
Total				2401

the original isolator. The new isolator was tested in the CHS at pump loads as high as 2 Kw and substantial performance improvements were observed. At a pump load of 1.5 Kw, the calculated pressure drop through the new isolator is 132 N/m^2 compared to a previous value of 1000 N/m^2.

Pressure drop in the pump is the second largest component shown in Table 3. In a higher capacity system the length of the pump will triple. This will increase the pump's vapor losses as the vapor flow is predominantly axial, and it will reduce liquid losses as the radial flow in the Porex dominates the pump's liquid pressure drop. The overall effect of the increased length will be to increase pump pressure loss as the vapor losses are greater than the liquid losses. One attractive feature of the grooved Porex pump is that the geometry of the vapor channels can be easily changed during the machining process to reduce the vapor loss. The current grooved Porex pump contains 36 vapor channels, each of which are 1.58 mm (.062 inches) deep and 0.75 mm (.028 inches) wide. The vapor pressure drop can be maintained at the current level despite the increased pump length if 30 vapor channels are used which are widened to 1.14 mm (0.045 inches). Further improvements can be achieved using even larger channels, but some consideration must be given to the reduction of contact area between the Porex and the pump body and its effects on liquid pressure drop and heat transfer. The groove geometry above maintains the same land width present in the current design.

In addition to investigating vapor channel modifications, the pump design effort also identified design improvements aimed

at increasing pump fabricability and reducing its sensitivity to liquid subcooling. A completely weldable pump was designed which features Bi-Braze aluminum/stainless steel transitions at either end and thermal isolation of the liquid-vapor seal from the pump's heat input zone.

Fabrication development of the new pump design was pursued to a point where the critical assembly steps were addressed. Insertion tests were performed to ensure that the Porex wick structure could be installed in the pump body. A 76 cm (30 inch) section of Porex was repeatedly installed in the same length pump body with a 0.29 mm (0.011 inch) diametrical interference fit. Welding tests were performed to ensure that the welded joints at the ends of the pump body could be made without destroying the Porex. Successful welds were made on the pump body within 6 mm (0.25 inch) of the Porex using liquid nitrogen chilled blocks. Visual examination of the Porex after welding showed no discoloration or distortion.

The remaining component pressure drops shown in Table 3 constitute approximately 30% of the total. In order to maintain adiabatic liquid and vapor pressure drops at reasonable levels, the line diameters must be increased to account for an increase in length by a factor of 3 and an increase in heat transport by a factor of 2.5. Since the flow in both sections are turbulent, the combined effects of these changes would increase the pressure drop by a factor of 15 if no changes were made. Liquid losses can be maintained at current levels by increasing the inside diameter of the line to between 1.3 and 1.5 cm (0.5 to 0.6

inches). The same increase should be made in the liquid subcooler. The vapor line diameter would need to increase to approximately 4 cm (1.6 inches) to maintain the same pressure drop, but an increase to 3 cm (1.2 inches) would probably suffice.

Pressure drop in the condenser section can be reduced by increasing the number of parallel passes and/or increasing the line size. The current condenser utilizes four parallel passes with a line diameter 0.77 cm (.30 inches). Increasing the number of parallel passes to six and the line diameter to 0.95 cm (.375") will keep the pressure drop the same.

With the component modifications described above, including the new isolator design and the modified pump, the total pressure drop in the increased capacity CHS should be even lower than in the current CHS at the current design level. Table 4 presents a comparison of calculated pressure drops on a component basis for the existing CHS at a total load of 6 kw and the high capacity system at a total load of 15 kw. Most of the component pressure drops are comparable except for the isolator, which emphasizes the difference between the original isolator design and the modified version which was fabricated and tested under Task 1.

Table 4

Existing CHS	High Capacity CHS
Q_{pump} = 1.5 Kw	Q_{pump} = 1.5 Kw
Q_{Total} = 6 Kw	Q_{Total} = 15 Kw
Transport Length = 10 m	Transport Length = 30 m
Pump Length = 0.30 m	Pump Length = 0.91 m

Component	ΔP (N/m^2)	ΔP (N/m^2)
Pump		
Vapor	632	632
Liquid	83	28
Isolator	1000	132
Adiabatic		
Vapor	123 (2.3cm)	473 (3.0cm)
Liquid	367 (0.77cm)	332 (1.4cm)
Condenser (50% active)	96 (4 passes,.77cm)	89 (6 passes,0.95cm)
Subcooler	100	90
---	---	--
Total	2401	1776

CONCLUSIONS AND RECOMMENDATIONS

The current program addressed several aspects of CHS performance. The major program accomplishments and conclusions are summarized below:

- The performance capabilities of the grooved Porex pump exceeds that of the grooved aluminum pump. The inherent flexibility in the vapor channel geometry afforded by the grooved Porex pump make it an ideal candidate for next generation pumps.
- A new isolator was designed, fabricated and tested which substantially reduced the pressure drop of the isolator. With the new isolator, transport limits of each pump exceeded 2 kw (heater limit) at 24 cm (9.5 inches) adverse elevation. Total system load at the same elevation exceeded 3.6 kw (cooling limit).
- Hybrid capillary/mechanically pumped systems were tested in both series and parallel configurations. Series hybrid systems are subject to temperature control problems resulting from reservoir deprime and pump flooding. Parallel hybrid systems are not nearly as susceptible to these problems, but the amount of augmentation provided by the mechanical pump is heavily dependent on the resistance in the loop's liquid phase.
- The demonstrated performance capabilities of a capillary pumped loop appear consistent with the requirements of higher capacity systems. Individual pump and isolator performance have already attained the levels

anticipated in larger systems. Provided longer pumps can be designed to minimize vapor losses and other loop components can be enlarged to reduce pressure drops, capillary pumped loops capable of 15 kw transport over 30 meter distances are feasible.

Throughout the course of the program, several areas were identified which merit further evaluation. It is recommended that the following items be pursued in a follow-on effort.

Continued Evaluation of Hybrid System

The hybrid tests which were performed during the current program were limited by practical considerations such as heater power and cooling limitations. As a result, tests were conducted at large adverse elevations and with flow restrictions (metering valve) in the liquid line in order to limit heat transport.

It is recommended that this effort be continued but with the practical considerations removed. One means to accomplish this is to perform the hybrid test on a CHS with more capillary pumps. This would enable system load to be increased without exceeding individual heater limits. New heater elements better suited for high power input should also be considered. Increased cooling capacity is also required. Additional instrumentation including more thermocouples on the capillary pumps and pressure transducers to characterize flow resistances should also be implemented.

Tests should be performed to evaluate both series and parallel hybrid configurations. Test variables should include adverse elevation and variable flow resistance.

Continue Development of Increased Capacity Pump

The design analysis conducted as part of this program indicates that the capillary pumped loop can meet the performance requirements of higher capacity systems. Fabrication development has shown that larger pumps present no inherent fabricability problems, and that fully welded pump designs are feasible.

It is recommended that the development effort for larger capacity pumps be continued. The next logical step would be to fabricate one or two full scale pumps and install and test them in an existing CPL. Following successful completion of this step, a large cold plate incorporating a multitude of large pumps would be fabricated and tested. The tests would be performed with a larger CPL test bed which incorporates larger liquid and vapor transport lines and a larger condenser to accommodate increased system loads.

Continued Investigation of CPL Performance Anomalies

Test results obtained during the current program revealed some as yet unexplained CPL behavior. In particular, the influence of adverse elevation on performance is not nearly as substantial as theory predicts. It is recommended that additional testing be directed toward explaining this anomaly.

One possible explanation for the lack of performance degradation with elevation is that the limits which are normally encountered during testing are not heat transport limits but heat flux limits (possibly nucleate boiling limits). After all, the typical failure mode is a gradual increase in pump temperature

above reservoir temperature, not a total deprime of the pump. And flux limits, although they are dependent on liquid stress, are not influenced in the same manner by adverse elevation as are heat transport limits.

It is recommended that the investigation be continued with this premise, and that tests be conducted to define heat flux limits and heat transport limits independently. These tests could be conducted with variable length pump heaters and would best be performed with long pump bodies as they provide ample evaporator area and hence permit wider variations in relative heat flux and heat load.